Distribution Category:
Safeguards—Nuclear Materials
Security (UC-15)

ANL-80-13
Volume III

ARGONNE NATIONAL LABORATORY
9700 South Cass Avenue
Argonne, Illinois 60439

FAST CRITICAL ASSEMBLY SAFEGUARDS: NDA METHODS FOR HIGHLY ENRICHED URANIUM

Summary Report
October 1978—September 1979

by

F. O. Bellinger and G. H. Winslow

Nondestructive Assay Section
Special Materials Division

December 1980

TABLE OF CONTENTS

LIST OF ILLUSTRATIONS

LIST OF TABLES

FAST CRITICAL ASSEMBLY SAFEGUARDS:

NDA METHODS FOR HIGHLY ENRICHED URANIUM

ABSTRACT

NDA methods, principally passive gamma measurements and active neutron interrogation, have been studied for their safeguards effectiveness and programmatic impact as tools for making inventories of highly enriched uranium fast critical assembly fuel plates. It was concluded that no NDA method is the sole answer to the safeguards problem, that each of those emphasized here has its place in an integrated safeguards system, and that each has minimum facility impact. It was found that the 185-keV area, as determined with a NaI detector, was independent of HEU plate irradiation history, though the random neutron driver methods used here did not permit accurate assay of irradiated plates. Containment procedures most effective for accurate assaying were considered, and a particular geometry is recommended for active interrogation by a random driver. A model, pertinent to that geometry, which relates the effects of multiplication and self-absorption, is described. Probabilities of failing to detect that plates are missing are examined.

NDA METHODS FOR HIGHLY ENRICHED URANIUM

by

F. O. Bellinger and G. H. Winslow

Nondestructive Assay Section

Special Materials Division

I. INTRODUCTION

The enriched-uranium portion of a fast critical assembly (FCA) fuel inventory typically consists of many thousands of individual fuel pieces fabricated in a wide range of sizes. Because the fuel is uranium metal of high enrichment, and because the fuel exists in such a vast numerical quantity, the inventory necessarily represents a prime diversion target for anyone dedicated to illicit intentions. Furthermore, the highly enriched uranium (HEU) fuel (as opposed to plutonium-containing fuel) may be easily handled in refabrication efforts such as casting, machining, and drilling, etc.--all of which adds to the diversion attractiveness of the material. The rapid and accurate nondestructive verification of the FCA-HEU vault-stored inventory can be a formidable task--especially under the conditions of a bona fide diversion alarm. Even under the normal inventory situations, the nondestructive verification methods must not greatly affect facility programs and operations. The objective of this work was to characterize the relative merits of several nondestructive assay (NDA) methods to understand how they may be used in an effective safeguards program for FCA-HEU fuel.

II. SAFEGUARDS PHILOSOPHY FOR FCA-HEU FUEL

A number of underlying principles have prefaced the investigative effort on HEU fuel verification methods. First, it is our contention that all NDA techniques, whatever their inherent limitations, in one way or another have a useful place and can be used effectively somewhere in the overall safeguards program. That is, no one single measurement method can be made to satisfy all aspects of a particular safeguards problem. Rather, a safeguards program, in order to be effective, must consist of an integrated network of physical security measures, precise record-keeping practices, sound administrative procedures, and, finally, practical NDA methods. This line of thought is necessary so that certain of the NDA methods are not needlessly discounted because the inherent limitations of the methods are not considered in the full safeguards context. Secondly, two broad levels of NDA technique may be defined--that is, those techniques that are rapid,but that are, perhaps, prone to certain diversion schemes, and those techniques that are time-consuming but that yield higher verification certainties. The time-consuming methods are, of course, more difficult to fit into the safeguard picture because they tend to have a large programmatic impact. The value of the more rapid NDA methods may be enhanced through the application of complementary measures such as weight verification plus tamper-indicating device (TID) inspection The more time-consuming methods may be aided by the use of carefully constructed sampling plans, or by a scheme of more-or-less continual application. Once the basic characteristics of a method are understood, the task becomes one of

carefully defining when, where, and how the NDA technique may be applied to the safeguards problem.

And, finally, it became apparent at the outset of the task that all of the vault-stored HEU material must be suitably contained before effective safeguards measures can be applied. Basically, the HEU plate canister must readily allow the nondestructive examination of the fissile content. When gamma radiometric methods are to be used, a four-sided viewing capability is necessary. For active-interrogator applications, a suitable plate-stacking geometry must be possible within the canister, and the canister itself must be dimensionally compatible with the active assay unit. Further, the canister must readily accept one or more TID's, and, when opened, must allow for a rapid physical inventory by way of an actual plate count. The canister storage practices must be such that each unit is readily accessible, so that unstacking (as in the case of "birdcages") is not necessary. In the case of unclad HEU plates, the canister must not be hermetically sealed to avoid gas-pressure buildup from uranium hydride. At the same time the container must be sealed to the extent that uranium-oxide particulates cannot escape and contaminate the storage facility. Much thought was devoted to the containment problem as a part of this effort, and the results will be presented in the future.

III. A SURVEY OF NDA METHODS INVESTIGATED

A. Gamma Radiometric Methods

Under certain situations it is possible to apply gamma radiometric

measurement methods to verify the integrity of FCA fuel canisters containing HEU plates. In this case, a verification action prompted by a sudden diversion alarm would call for a rapid determination of the likelihood of a major diversion of fuel from the FCA storage facility. A spectroscopic analysis shows that there is no major fission-product gamma-ray interference in the immediate neighborhood of the characteristic 185-keV photopeak of ^{235}U for HEU plates as typically irradiated in subcritical assemblies. It is possible, therefore, with proper background-subtraction methods, to obtain an integrated area for the 185-keV peak that is independent of the irradiation history of the FCA fuel. Furthermore, the verification task may be accomplished with a sodium iodide (NaI) detector so that simplified electronics may be used, and so that a large canister throughput is possible. Diversion schemes involving plate removal, substitution, and rearrangement were studied. Obvious possible complications in data interpretation caused by self-absorption effects are minimized through the use of TID's, by the overall safeguards administrative procedures, and by the storage canister design.

B. Active Interrogator Method

The random driver may be used to verify the contents of HEU plate storage canisters. Here, a source of uncorrelated neutrons is used to induce fission events in the ^{235}U portion of a sample material. Plastic scintillation detectors are used to convert the induced-fission radiation to electronic pulses, and fast-coincidence logic circuitry is then used to separate the correlated fission-related events from the

uncorrelated background events. The ultimate output, then, is a coincidence count that is proportional to the fissile mass of the sample. An HEU plate-stacking geometry was selected on the basis of the form of the calibration curve that resulted from a plate-by-plate assembly of fuel. The selected stacking geometry eventually dictated the general form of the storage canister design. The HEU plate diversion sensitivity of the method was examined for plate removal and substitution. A mathematical model describing experimental results was constructed with the differential response curve obtained by migrating enriched plates through a stack of depleted plates of the same dimension.

The effect on the random-driver response from fission-product gamma radiation from plates having a recent reactor-use history was studied. The adverse effects of fission-product gamma radiation on the coincidence response were verified and were shown to persist for as long as three weeks following the irradiation. It is important, however, to note that, by observing the passive 3/4 coincident count and by comparing that count with the average of such counts from an unirradiated canister, one can easily tell if there are irradiated plates in the canister. Attempts to shield the fission-product radiation from the detectors by using extra lead were only partially successful. A gamma-gamma coincidence rejection scheme was attempted, and, again, the technique proved helpful but was not sufficient to reduce the fission-product gamma component to negligible quantities.

C. Active Well Counter

A brief attempt was made to fashion an active well counter from an existing neutron coincidence well counter (NCWC). This method holds promise for application to the verification of irradiated plate canisters since the neutron detectors used in the NCWC are not particularly sensitive to gamma radiation. We feel the method has merit and should be thoroughly investigated, but, unfortunately, the necessary resources were not available for us to make a fair evaluation of the method at this time.

D. Delayed Neutron Counter

Another approach to the problem of measuring irradiated HEU plates is to make use of the delayed neutrons from induced fission events. A straightforward experiment was conducted that verified the feasibility of the idea, and, indeed, it has been shown by others to be a viable technique for NDA applications. A full evaluation of the method for FCA purposes was beyond the scope of our current resources.

IV. EXPERIMENTAL RESULTS FOR GAMMA RADIOMETRIC METHODS

A. High-Resolution Gamma Spectra

At the outset, a possible fission-product gamma-ray interference problem was anticipated. In order to study the matter further, a high-resolution spectrum from an irradiated HEU plate was compared with that

of an unirradiated plate. The region of predominant interest is, of course, centered around the 185-keV peak from ^{235}U. An Ortec low-energy intrinsic detector having resolution characteristics of 332 eV FWHM at 5.9 keV and 585 eV FWHM at 122 keV was used for this work. A Nuclear Data 4410 computer-based analyzer was used to collect and process count data. A peak-extraction overlay program was used. After calibration, this program performs a peak search; then it assigns an energy to each peak and calculates a peak area corrected for Compton background. Table I summarizes the results of the high-resolution spectrum analysis. The 185-keV region is worthy of a brief discussion. Blachot and DeTourreil[1] list Pm-151 and Sb-124 as fission products which have photon emissions that would interfere with the 185.7 keV from ^{235}U. However, in each case one should also see the most prominent peaks of 340.1 keV for Pm-151 and the 602.7 keV for Sb-124 if, indeed, these isotopes were present in the HEU plate to any great extent. These peaks were not present in the spectrum obtained from the irradiated plate. In summary, then, the dominant radiation is from the ^{235}U isotope, and, since the region around the 185-keV peak is clear of interference photopeaks, one may use a high-quality NaI detector system to view HEU plates and canisters.

B. Sodium-Iodide Detector Spectra

A 2" x 2" Harshaw sodium-iodide detector having a resolution of 20-keV FWHM at a count rate of 2×10^5 counts/min was used to study the 185-keV region of ^{235}U. Compton background was subtracted by calculating the straight-line average at channels adjoining the

TABLE I. High resolution spectrum analysis of an irradiated HEU plate.

Gamma Energy (keV)	Interpreted Counts *	Isotopes
143.73	69,236.12	U-235
163.42	24,401.75	U-235
185.70	267,639.24	U-235;Pm-151(28h);Sb-124(60d)
194.9	2,843.8	U-235
205.3	31,312.6	U-235
228.6	7,349.8	Te-132(3.2d)
293.4	1,844.1	Sb-127(2.2h);Sb-127(3.87d);Ce-143(32.7h)
328.8	1,650.4	La-140(1.7d)
364.9	3,715.4	I-131(8.05d)
486.9	2,338.1	La-140(1.7d)
530.6	222.1	I-133(21h)
537.3	1,080.2	Ba-140(12.8d)
630.0	266.1	Pm-148(43d)
667.6	2,731.1	Sb-127(3.9d)
724.1	936.5	Zr-95(65d);Pm-148(43d)
756.5	860.8	Zr-95(65d)
765.5	1,410.3	Nb-95(35d)
772.3	1,378.3	Pm-151(28h);Te-131(28.8h)
815.6	457.0	La-140(1.7d)

* Integrated counts are not corrected for detector efficiency or self-absorption in HEU plate.

photopeak on either side. Table II shows the integrated, background-subtracted, photopeak area for both irradiated and unirradiated 2" x 3" x 1/16" HEU plates viewed by a NaI detector at a source-to-detector distance of 40 cm. Column 4 of the table shows the ratio of irradiated to unirradiated plate peak areas. Here, it is clearly seen that the 185-keV photopeak area is independent of the HEU plate irradiation history.

C. HEU Fuel Verification with a NaI Detector

Two options exist for using NaI detectors for the verification of FCA-HEU fuel. These options are 1) the verification of individual plates, and 2) the verification of a stacked assembly of plates in a storage canister. Regarding the latter approach, two further possibilities exist---namely, to survey the entire stack as a unit or to perform a plate-by-plate high-resolution slow scan of the stack.

If option 1 is to be used (i.e., the plates viewed individually), an automated fuel-handling system with an assay counter station would almost be a necessity. Such a system is currently being designed and is expected to incorporate other safeguards measures such as automatic sample weighing and automatic canister identification. To complete the automated system, an on-line link to a suitable computer would be necessary. Self-absorption effects could be minimized by having NaI detectors view both top and bottom surfaces of each plate. In this way, an adequate verification could be performed on HEU plates up to 1/8" thick.

TABLE II. Photopeak area for irradiated and unirradiated HEU plates.

	Peak Area		
Count Time (sec)	Irradiated Plate	Unirradiated Plate	Ratio
1	4708	4899	0.96
3	14171	14535	0.97
5	24044	23034	1.04
10	48600	47945	1.01
30	144013	149391	0.96
60	288821	293413	0.98

Figure 1 shows the ratio of the standard deviation $\sigma(A)$ to the background-substracted peak area A as a function of count interval. For this data, a single 2" x 3" x 1/16" unirradiated HEU plate was viewed by an NaI detector on one surface only. The figure shows, for example, that a count interval of 5 seconds is sufficient to yield a precision of about 1%.

Option 2 allows one to verify a stack of HEU plates while they are stored in the canister. By using multiple NaI detectors, or, possibly, by rotating the canister and using a single NaI detector, all four edges of the stack may be examined. Figure 2 shows a calibration curve of the integrated 185-keV peak (background-subtracted) vs the number of 2" x 2" x 1/16" HEU plates in the canister. Plate removal, or substitution with nonfissile materials, is detected as a reduction in count level from that expected from a fully loaded canister. However, because of self-absorption effects, a plate rearrangement following plate removal is possible such that the count of a fully loaded canister is approximated. It is important to note that the threat from this type of diversion scheme may be considerably lessened through a procedure of canister weighing and through the effective use of TID's. An outsider (i.e., one not normally associated directly with the storage facility) would find it extremely difficult to gain access to the storage facility, obtain the necessary NDA counting equipment, and have time to "experimentally" adjust the count from a container after the diversion. An insider, on the other hand, would find it somewhat easier to perform these diversion functions; however, the administrative practices

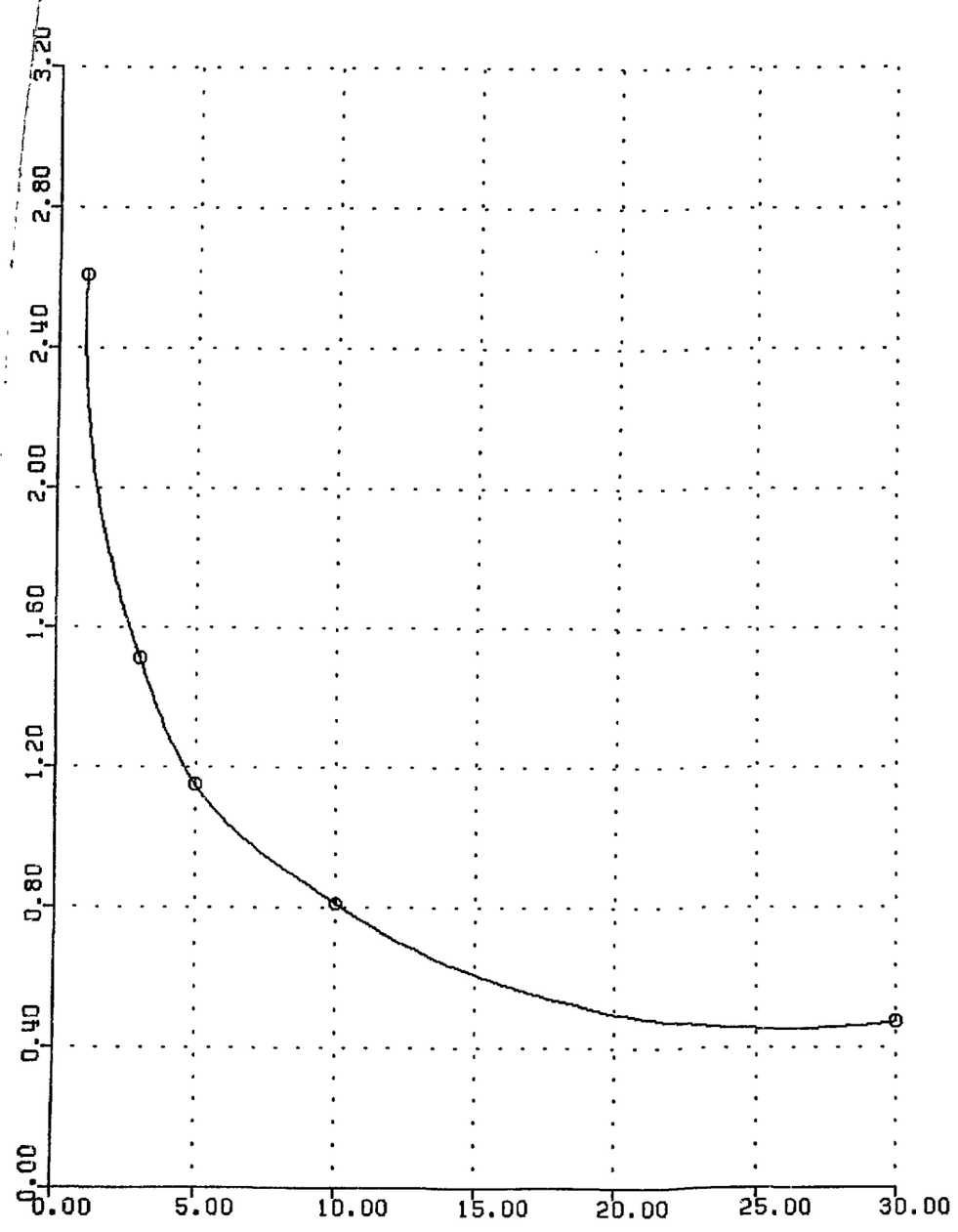

Fig. 1. Ratio of the standard deviation in the net peak area to the area as a function of count interval. For these data, an NaI detector was used to view a single surface of a single 2" x 3" x 1/16" unirradiated HEU plate.

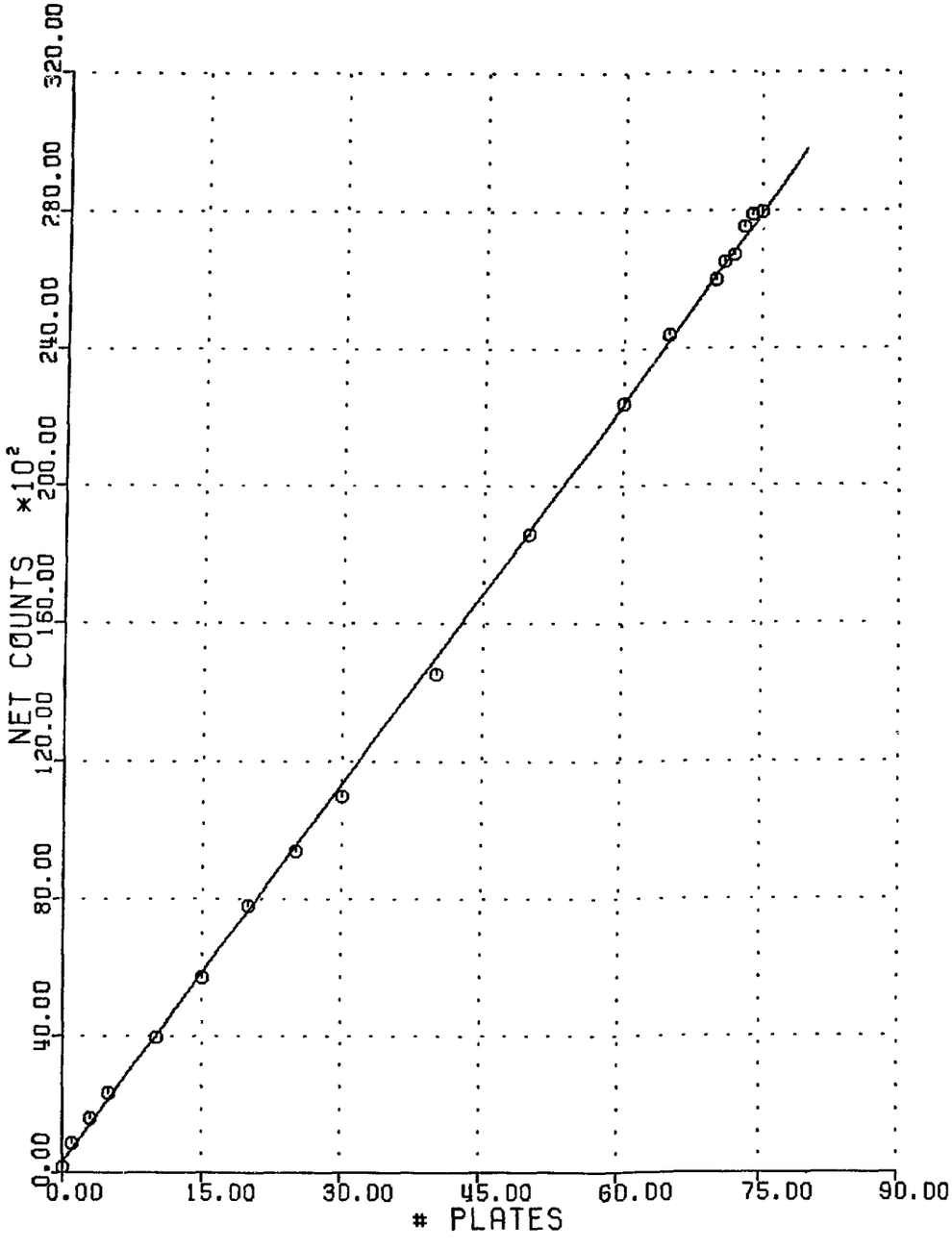

Fig. 2. Calibration curve for NaI detector. Shown are the counts in the integrated, background-subtracted 185-keV peak vs. the number of 2" x 3" 1/16" HEU plates in the canister.

associated with vault physical-control measures reduce the threat to unlikely proportions. If a diversion by this method is successfully perpetrated by an insider, a great deal more than the NDA method has failed!

The slow-scan, highly collimated detector version of option 2 was found to have little merit in terms of item throughput, and, therefore, may be discounted from an effective safeguards plan. Plate measurement resolution was acceptable for the 1/16"-thick HEU plates, but serious doubt exists for the technique performance when it is applied to thin plates.

V. RANDOM DRIVER METHODS FOR UNIRRADIATED PLATES

A. Introduction

The instrument used was the National Nuclear Random Driver. The most extensive tests were made with 2" x 2" x 1/16" fast critical assembly fuel plates; additional checking was done with 1" x 2" x 0.026" plates and 2" x 3" x 1/16" plates. The maximum numbers of plates involved in one test on these different sizes was 75 (5.14-kg ^{235}U), 180 (2.5-kg ^{235}U), and 50 (5.17-kg ^{235}U), respectively. The experiments included substitution of one, or of two, dummy plates of depleted uranium (DU), aluminum, or plexiglass for HEU plates.

Two loading geometries were investigated. One in which the plates stood vertically in the driver, and were stacked horizontally, was

quickly rejected in favor of one in which the plates were laid flat in the driver and stacked vertically. Some of the reasons are evident in Fig. 3, where curve a is a typical result for the first of these geometries, and curve b is a typical result for the second, with 2" x 2" x 1/16" plates and a table height of 7-7/8". The points plotted for each of these curves are averages of five 100-sec counts. In each case, of course, the plates were held in an appropriately shaped container. With the first of these geometries, the curve of gross count vs number of plates was roughly of the form of two straight lines, but it was not qualitatively reproducible. The location and nature of the connection between the two sections did not repeat, and we found excessive variance in one or the other, or both, of the two legs. We will not report further on results using this geometry.

When the plates lie flat and are stacked vertically, cylindrical symmetry is maintained, and the problem of excess variance is reduced to a minimum, provided the driver is used in the 3/4 coincidence mode. The curve of gross count vs number of HEU plates is smooth and, while it was not quantitatively the same on every day of testing, it always had the same form. Because of this, and the symmetrical loading pattern, it was possible to develop a model by which that curve can be reproduced, and which provides a physical explanation for the results observed in the substitution experiments. The line drawn as curve b in Fig. 3 is from that model.

Brief tests were made with the driver in the 2/4 coincidence mode, since the increased count rate would reduce testing time. Again,

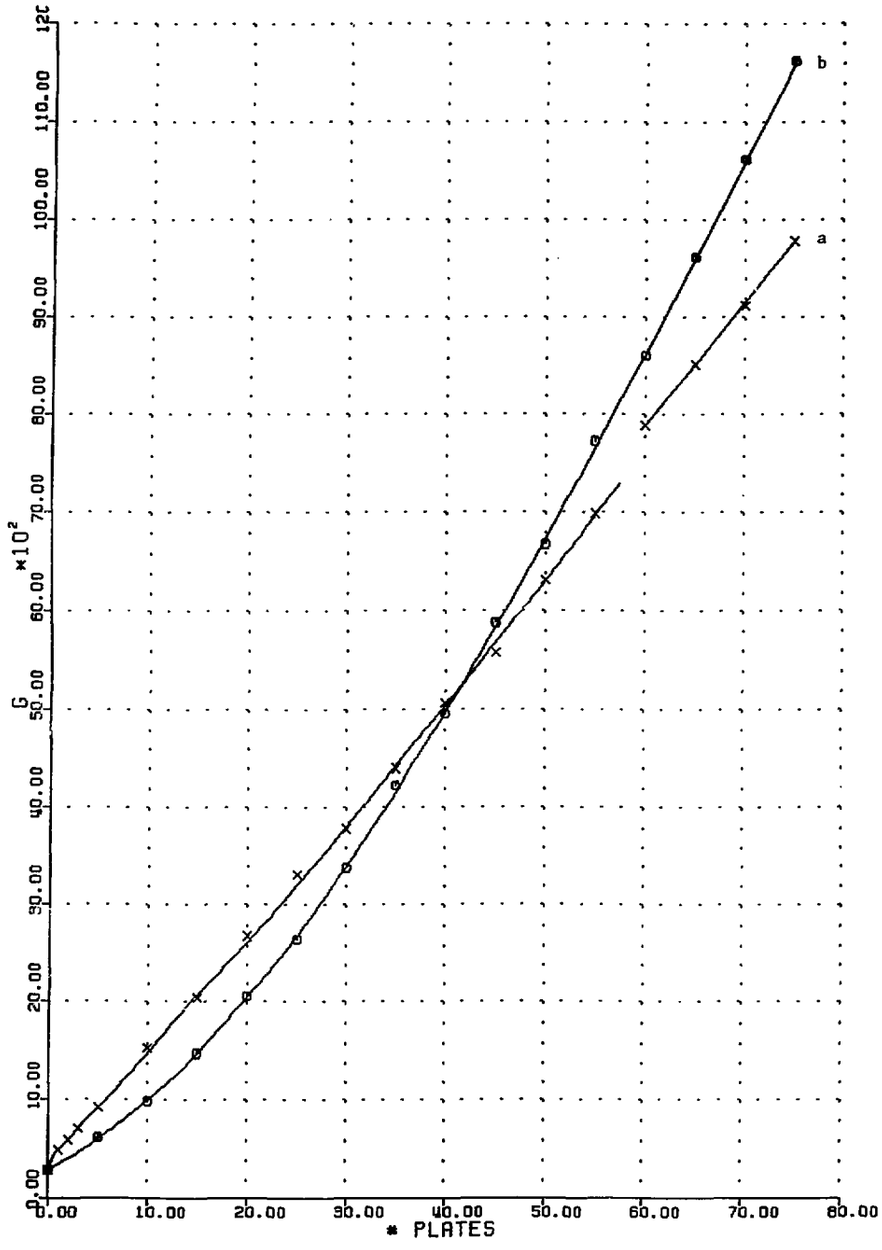

Fig. 3. Comparison of random driver counts for two 2" x 2" x 1/16" plate loading geometries. For curve a, the plates stood vertically and were stacked horizontally. For curve b, the plates lay flat in the container and were stacked vertically.

however, excess variance occurred more frequently than we would expect, and the actual assay values on stacks with substituted plates frequently were greater than the known number of HEU plates. We do not profess to understand this result.

The presence of fission-product gamma radiation has been found to seriously jeopardize the correct interpretation of the random driver count data when no extra shielding is used. The presence of one or more irradiated plates that would produce this gamma radiation can be detected by measurements in the passive mode. Such a test should precede an active mode verification count.

In the following sections we discuss the statistical methods used, the results of measurements in the 2/4 coincidence mode, the general characteristics of the preferred testing procedure, the mathematical model for the latter, and the results of the substitution tests with the latter.

B. Statistical Procedure

The principal aspects of the statistical procedures used are to be found in Section III of Volume II, ANL-80-13.[2] We add here estimates of the probability of committing the Type-II error of failing to detect that plates are missing. These numerical estimates are pertinent only to the HEU plates in the preferred geometry. We mention again, here, that the Type-I error is a conclusion that plates are missing when none are.

The significance level, α, of the test described in Volume II is 0.05. Thus, the probability of committing a Type-I error is 0.05. Correspondingly, there is a probability, β, of committing the Type-II error of accepting $p = p_0$ when, in fact, $p < p_0$. Its value depends on α, the variance in A, and the size of $p_0 - p$. That is, for given α and $\sigma(A)$, one is much less likely to fail to detect that $p_0 - p = 2$ than that $p_0 - p = 1$.

Values of β are given by so-called operating characteristic (OC) curves in which, for the particular distribution of interest, β is plotted against the ratio of the difference being looked for to the standard deviation in a single observation (or observation of unit weight) for varying numbers of observations. While we use a normal distribution, based on the usual expectation that there will not be variance in addition to that from the counting statistics, we cannot use the usual OC curves because there are two contributions to the variance in A. The following procedure has been worked out for the calculation of β for a given calibration curve and varying numbers of observations on the test stack.

The upper end of curve b of Fig. 3 turns out to be accurately linear over a much greater range of p than required for our substitution experiments. Thus, we used such a first-order calibration curve for those tests. If the slope is b, independent of the assay, A, the value of the standard deviation, σ, in A will be

$$\sigma = [b^2 S_c^2 + \bar{G}/n]^{1/2}/b$$

where $\bar{G}$ is the average of n observations on the test stack and S_c^2 is defined in Section III of Volume II, ANL-80-13.[2] With this value of σ we can use the standard OC curve for a one-sided normal test at $\alpha = 0.05$ and a single observation by finding β at the abscissa, $(p_0 - p)/\sigma$. As an example we use, for $\bar{G}$, values of G calculated from the first-order equation fit to the range of curve b of Fig. 3 from $p = 55$ to $p = 75$. The value of the slope is 192.87 counts per plate, $b^2 S_c^2 = 1901$, and, at 74 plates, $G = 11355$. Then the probabilities of failing to detect that a single plate is missing, for various values of n, are given in Table III. Even with a single observation, the probability of failing to detect that two plates are missing is 0.04.

It must be pointed out that these values of β apply only to the detection of missing plates. As will be shown later, substitution lowers the count by more than does the simple removal of an equal number of plates, and by varying amounts depending on the position in the stack at which the substitution was made. Thus, the values of β are, in effect, lowered by substitution, but no useful assessment of such lowering can be made since it would not be known where in the stack substitution might have been made.

It should be mentioned that the probability of committing a Type-II error, with the same counting effort, can be lowered by increasing α. This would have the effect, of course, of increasing the false alarm rate.

Curve b of Fig. 3 can be fit by a cubic, and its upper end is where

TABLE III. Probability of failing to detect that $p_o - p = 1$.

n	$1/\sigma$	β
1	1.68	0.49
2	2.22	0.28
3	2.56	0.18
4	2.80	0.12
5	2.99	0.09
6	3.13	0.08
7	3.25	0.05
8	3.35	0.04

the curvature is changing sign. This fact, plus investigations with the model to be described later, indicate that the upper end of the curve would be concave downward were the table height greater than the 7-7/8" used here. Thus, for greatest simplicity of calculation, there is an optimum table height.

C. 2/4 Coincidence Mode Results

In general, the substitution tests were made by inserting one, or two adjacent, dummy plates of equal size in place of the same number of HEU plates at positions roughly 1/4, 1/2, or 3/4 of the distance up from the bottom of a full stack. These positions will be designated B, C, and T, respectively.

The brief series of 2/4 coincidence mode tests were made with the 2" x 2" x 1/16" plates and plexiglass dummies. Two calibrations were made. Calibration I was a complete curve which appeared to be linear within the large scatter. Calibration II was made only for the top five points from 55 to 75, with observations in each case at every five plates. Three 10-sec observations were made of each of the calibration points, and five observations were made for each of the six substitution tests. The variance was much larger than to be expected from counting statistics for the full curve, but not for any of the other measurements. For the Calibration I results in Table IV, only the top five points were used. In this table, and subsequent tables of this sort, p is the number of HEU plates in the stack, M is the substituted material, P is the substitute position in the stack, A is the assayed

TABLE IV. 2/4 coincidence mode substitution tests. 2" x 2" x 1/16" plates; $n_0 = 75$

p	M	P	A	LE	E
			Calibration I		
74	Plex	B	73.91	2.31	II
73	"	B	73.87	2.30	II
74	"	C	72.84	2.16	II
73	"	C	72.74	2.15	0
74	"	T	74.05	2.08	II
73	"	T	75.39	2.53	II
			Calibration II		
74	Plex	B	75.39	1.10	II
73	"	B	75.35	1.10	II
74	"	C	74.23	1.06	II
73	"	C	74.12	1.06	II
74	"	T	75.55	1.11	II
73	"	T	77.01	1.17	II

number of plates, LE is the one-sided 95-percent CL error, and column E shows the type of conclusion error, I or II. A zero in column E means the correct conclusion was reached. The entries in column E of Table IV show clearly why we abandoned the 2/4 coincidence mode for this work.

D. Characteristics of Preferred Test

As is clear from the previous sections, this test is to be made with the plates lying flat, one on top of another, with minor variations. For instance, we used the same rack for 1" x 2" plates, by putting two side by side in one layer, as for 2" x 2" plates. With the smaller plates, one, or two adjacent, layers contained the dummy substitutes, so that either two or four, rather than one or two dummies were substituted for a like number of HEU plates. The driver is to be used in the 3/4 coincidence mode; 100-sec counts were made for these experiments.

There is a height effect when the interrogating sources are in the positions we standardly use. That is, a unit of five HEU plates, for example, moved up through a stack of DU plates, one unit at a time, causes a response which is second order in the position in the stack. This curve is the bottom one of Fig. 4. If i is the position, with i = 1 at the bottom, the net count is given by

$$N_i = a_0 + a_1 i - a_2 i^2 \qquad (1)$$

which we describe as the "differential response curve." It is also

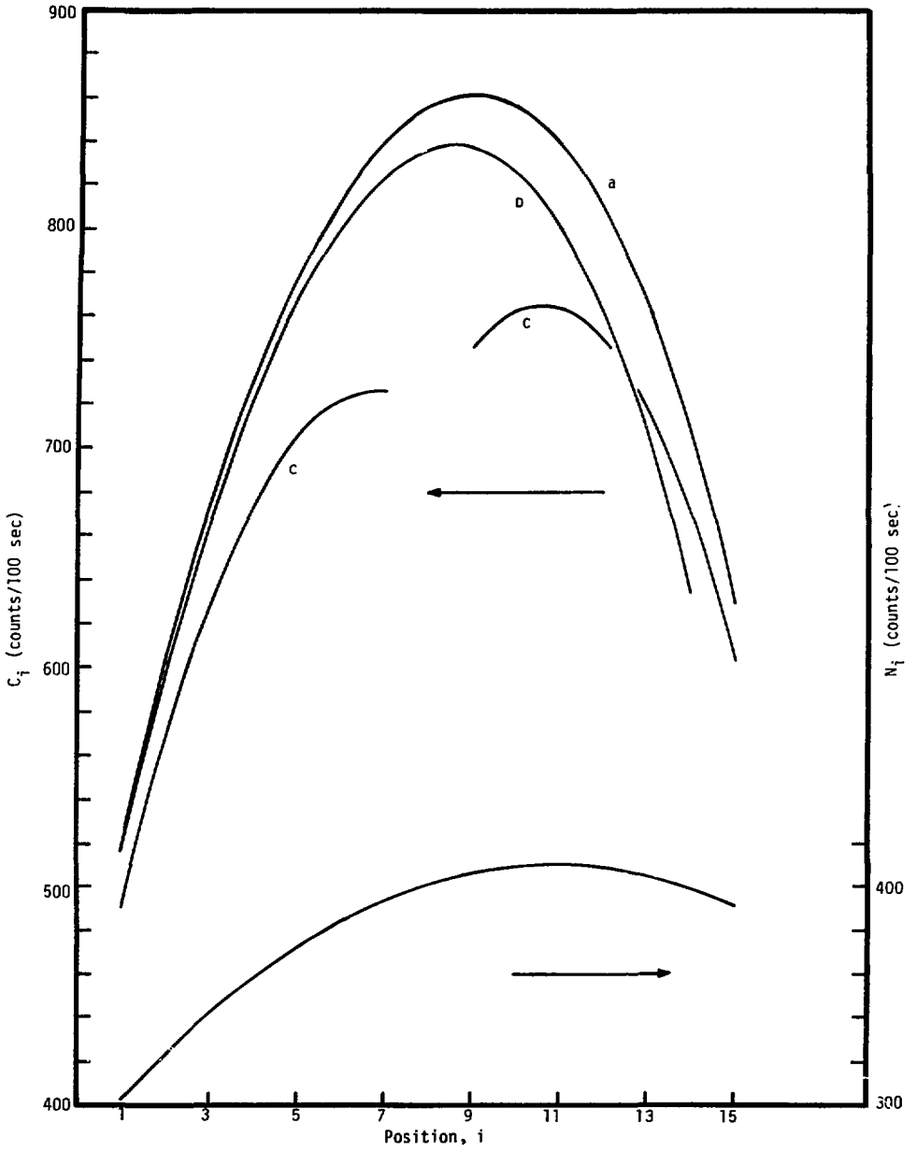

Fig. 4. Model derived curves for active counting of a vertical stack of horizontal plates. The lower curve is the differential response curve, the response of a five-plate HEU unit vs. its position in a stack of DU plates. The upper curves are responses per five-plate unit vs. the position of the unit in a stack of HEU plates. Curve a is for 15 such units, while curves b and c are for 14 such units and a single, substituted DU unit. The latter is at position 15 for curve b and at position 8 for curve c.

found, however, that when n successive units of five HEU plates are stacked, the resultant net count is considerably larger than

$$N = \sum_{i=1}^{n} (a_0 + a_1 i - a_2 i^2)$$

although we have found that the actually observed net count can be well fitted by an equation cubic in n, which N would be.

Experimental observations are "tainted" by statistical variation but, within that variation, the results of substitution of inert plates for HEU plates appear to depend on the place in the stack at which the substitution is made. When substitution is made well within the stack rather than near the top or bottom, the loss of count is definitely greater than for the mere removal of an equal number of plates, and, though less pronounced, the effect persists as substitution approaches either end of the stack. Such an effect, if it can be shown to have reality rather than being a statistically produced happenstance in our particular experiments, enhances one's ability to detect substitution.

E. Mathematical Model

A model has been constructed to "explain" the actually observed responses from a stack. It is based on the five-plate unit and has not been particularized to single plates, nor tested by comparison with experiment for substitution of five plates. When used to calculate the

effect of substitution of five plates, however, the results are, qualitatively, the same as the observed effects of single or double plate substitution. Since this effect has an important bearing on the reliability of detection of substitution, the model will be described.

It is assumed that the total response, C_i, from the ith unit in the stack is the sum of that due to the interrogating sources in the driver, N_i, and that due to interrogating sources presented by the other units in the stack. It is assumed that this additional response is some constant fraction of the additional source strength present at position i. Were there no absorption by intervening units, it is assumed further that the additional response at position i, caused by the unit at position j, could be represented as fC_j. Thus, sources adjacent to position i produce the additional response $f(C_{i+1} + C_{i-1})$. Sources farther away, however, are attenuated by the presence of the intervening units. If the transmission of a unit is g (which probably includes, also, effects of moderation), we finally write

$$C_i = N_i + f(\ldots + g^2C_{i-3} + gC_{i-2} + C_{i-1} + C_{i+1}$$

$$+ gC_{i+2} + g^2C_{i+3} + \ldots).$$

For instance, with a stack of three units,

$$C_1 = N_1 + f(C_2 + gC_3)$$

$$C_2 = N_2 + f(C_1 + C_3) \qquad (2)$$

$$C_3 = N_3 + f(gC_1 + C_2)$$

and the total net count is $C_1 + C_2 + C_3$. If f and g are known, and if the differntial response curve, Eq. 1, has been determined, all such simultaneous equations as Eq. 2 can be solved. It should be emphasized that application of the model does not depend on the particular form of the differential response curve found here. All that is required is a set of appropriate, tabulated values of N_1.

We put a least squares equation, cubic in n, the number of five-plate units, through the (this time equally weighted) integral response data for 2" x 2" x 1/16" plates that was used to test the model. We slightly adjusted the constant, a_0, in Eq. 1 so that N_1 would agree with the first net count from the least squares equation for the integral response; backgrounds vary slightly and not every five-plate unit is exactly the same as every other one. We evaluated f and g by fitting to the net count from the cubic integral response equation at n = 10 and 15 (50 and 75 plates, respectively). The values found were f = 0.09356 and g = 0.69822. The sum of squared residuals between the model calculations and the original data was about twenty percent greater than that sum for the least squares cubic equation. This is quite close enough for the purpose of testing the position effect of substitution. While the model is simple in concept, it would be

cumbersome for routine use as an assay tool, so that more erudite methods for evaluating f and g are not warranted.

In the stack of three units, had the one at position 2 been a dummy of the same absorption characteristics as an HEU unit, such as a DU unit, the responses would have been given by

$$C_1 = N_1 + fgC_3$$

$$C_3 = N_3 + fgC_1$$

and the total net response would be $C_1 + C_3$. But these are, respectively, smaller than the C_1 and C_3 obtained when the stack contained three HEU units. More to the point, when the substitution has been made,

$$C_1 + C_3 = (N_1 + N_3)/(1 - fg)$$

while, for a stack of two HEU units, only,

$$C_1 + C_2 = (N_1 + N_2)/(1 - f)$$

and, even though $N_3 > N_2$, $C_1 + C_3 < C_1 + C_2$. That is, the stack of two HEU units and a dummy at position 2 counts lower than a stack of two HEU units. Thus, the absorption-modified multiplication enhances one's ability to detect a substitution.

In our tests, the table height in the random driver was such that the maximum value of N_i was reached at a position above the center of a complete stack of 2" x 2" x 1/16" plates. This stack contained 75 plates, 15 five-plate units, and, for it, the calculated values of C_i follow a slightly distorted parabolic curve with its peak somewhat above the center of the stack. Thus, there is a position effect on substitution. Substitution near the center of the stack causes a greater loss in response than substitution near the top or the bottom, and substitution near the top causes a greater loss in response than substitution near the bottom. These effects are illustrated by the three upper curves, values of C_i, in Fig. 4. Of these, curve a is for a full stack of 15 HEU units, curve b is for substitution at position 15, and curve c is for substitution at position 8.

F. 3/4 Coincidence Mode Results

A characteristic of this preferred procedure, implied by previous discussion, is the rarity with which we observed variance, as indicated by the F-ratio tests, in excess of what we would expect from counting statistics. In addition to the reproducible geometry, and these well-defined objects, this implies good circuitry and good background conditions. Such considerations allow us to associate the high variances observed when the plates stood vertically in the driver and were stacked horizontally with poorly reproducible geometry, but we are at a loss to explain the high variances which occurred with the preferred geometry and the 2/4 coincidence mode, where both s_e^2 and s_ℓ^2 were larger than $\bar{G}_{max}$ by more than the critical value at the 95-

percent CL. (See Section III in Volume II of this report.)

In Table V we show a repeat of Table IV, except done in the 3/4 mode with 100-sec counts. Again, the same set of observations on the substituted stacks is used with each calibration, and all the work was done on the same day, though the substituted stack observations and Calibration II were closer in time than was either to the time of Calibration I. The differences in columns A and E are due to a systematic difference in the two calibrations, neither of which showed internal evidence of variance greater than expected from the counting statistics. For example, at 74 plates, the difference in the predicted values of G from the two curves is 157.4 with a standard deviation of 61.4. Thus, the difference is significant at the 95-percent CL. Further work on this project should include an investigation into the causes of such systematic differences.

The remainder of the results on the 3/4 coincidence mode tests are shown in Table VI. If we include only the Calibration-II results from Table V, 36 substitution trials were made, and three Type-II errors occurred. All of these were at single plate substitutions, and one was caused by excess variance in the count on the test stack. For the other case where there was excess variance and a Type-II error, A was sufficiently large that the error would have been made even at the expected variance. In these particular trials, the only one where a Type-I error could have occurred was at the first one in Table VI, where a count of a full stack was made in addition to the one used in the calibration.

TABLE V. 3/4 coincidence mode substitution tests. 2" x 2" x 1/16" plates; $n_0 = 75$.

p	M	P	A	LE	E
			Calibration I		
74	Plex	B	73.80	0.99*	0
73	"	B	72.22	0.87*	0
74	"	C	73.03	0.53	0
73	"	C	71.37	0.50	0
74	"	T	73.77	0.55	0
73	"	T	72.04	0.63	0
			Calibration II		
74	Plex	B	74.65	1.05*	II
73	"	B	72.98	0.92*	0
74	"	C	73.84	0.57	0
73	"	C	72.09	0.54	0
74	"	T	74.62	0.59	II
73	"	T	72.80	0.55	0

* For sample, $s^2/G > F_{0.05}(m - 1,\infty)$

TABLE VI. 3/4 coincidence mode substitution tests.

p	M	P	A	LE	E
2" x 2" x 1/16" plates				n_0 = 75.	
75	--	--	75.64	0.73	0
73	Al	B	72.66	0.67	0
74	"	B	73.72	0.69	0
73	"	C	71.52	0.65	0
74	"	C	73.40	0.68	0
73	"	T	71.81	0.65	0
74	"	T	73.52	0.69	0
74	"	B	74.17	1.06*	II
73	"	B	73.23	0.59	0
74	"	C	73.57	0.60	0
73	"	C	72.13	0.56	0
74	"	T	73.66	0.60	0
73	"	T	72.28	0.57	0
74	DU	B	73.79	0.60	0
73	"	B	72.69	0.58	0
74	"	C	73.65	0.60	0
73	"	C	71.39	0.55	0
74	"	T	74.04	0.61	0
73	"	T	72.07	0.56	0
1" x 2" x 0.026" plates				n_0 = 180	
178	Al	B	176.80	1.42	0
176	"	B	176.53	1.41	0
178	"	C	175.73	1.39	0
176	"	C	174.39	1.38	0
178	"	T	175.70	1.39	0
176	"	T	175.65	1.38	0
2" x 3" x 1/16" plates				n_0 = 50	
49	DU	B	48.48	0.31	0
48	"	B	47.53	0.30	0
49	"	C	48.21	0.30	0
48	"	C	47.19	0.30	0
49	"	T	48.46	0.31	0
48	"	T	47.00	0.31	0

* For sample, $s^2/G > F_{0.05}(m - 1,\infty)$

For the first seven entries under 2" x 2" x 1/16" plates in Table VI, and for those under 2" x 3" x 1/16" plates, three observations were made on each test stack. For the others, five observations were made.

Of the 36 substitution trials mentioned above, $A < n$ in 31. The average values of $(A - n)$ are shown in Table VII. These parallel the count loss as a function of position described in Section E. Were this tendency not present, the sensitivity to loss would be decreased; more Type-II errors would have occurred.

VI. RANDOM DRIVER METHODS FOR IRRADIATED HEU PLATES

A. Additional Lead Shielding

These experiments were done with 3" x 2" x 1/16" plates that had only cooled overnight after removal from the reactor. They had been subjected to a complex radiation history prior to removal, and were taken from a high-flux region. They were placed flat in the RD and stacked one on top of another. Unirradiated plates used for comparison had been out of the reactor at least five months.

It was found that the addition of an inch thick lead shield surrounding a single irradiated HEU plate countered adverse effects from the fission product gamma radiation to within statistical variation, as shown by the net counts given in Table VIII. Six 100-sec background counts were made before the plate counts and three were made afterwards. No significant background change was observed. All the plate count

TABLE VII. Average (A - n).

	2" x 2" x 1/16"	1" x 2" x 0.026"	2" x 3" x 1/16"
B	-0.014	-0.335	-0.495
C	-0.801	-1.940	-0.800
T	-0.401	-1.325	-0.770

averages were of three 100-sec counts. It is also apparent in Table VIII that the passive count is an indicator of recent irradiation.

Unfortunately, demonstrably for as few as 10 irradiated plates, and, we estimate, even for as few as two such plates, the extra shielding proved inadequate to remove all the excess count. For example, the net passive count for 10 irradiated plates was found to be nearly nine times that for 10 unirradiated plates when the extra shielding was used in each case. The ratio of the net active counts for that setup was nearly three.

Although the scatter was much greater than we generally expect, probably related to the rapid initial decay of the excess count, we found, with measurements on 1, 4, 6, 8, and 10 irradiated plates with the additional shielding, that both the passive and active counts exhibited the behavior described in Section V as being due to multiplication and absorption. In addition, we show, in Fig. 5, the difference between the net active and passive counts, the induced count, I, for these plates and for 10 unirradiated plates, again with the extra shielding, as curves a and b, respectively. Conceivably, but not demonstrably, multiplication could also be occurring in I for the irradiated plates.

We did not track these plates in time nor have we located the source of the low, but surprising and statistically real passive count on the unirradiated plates. One such plate showed a net count of 72.4 $\pm$ 8.7 without additional shielding and 23.0 $\pm$ 7.6 with the extra

TABLE VIII. Compare single irradiated and unirradiated plates.

	Unirradiated	Irradiated
	No additional shielding	
N_{act}	300.8 ± 13.8	1289.0 ± 19.7
N_{pass}	72.4 ± 8.7	755.2 ± 14.6
	Additional shielding	
N_{act}	88.6 ± 11.4	89.2 ± 11.4
N_{pass}	23.0 ± 7.6	30.0 + 7.7

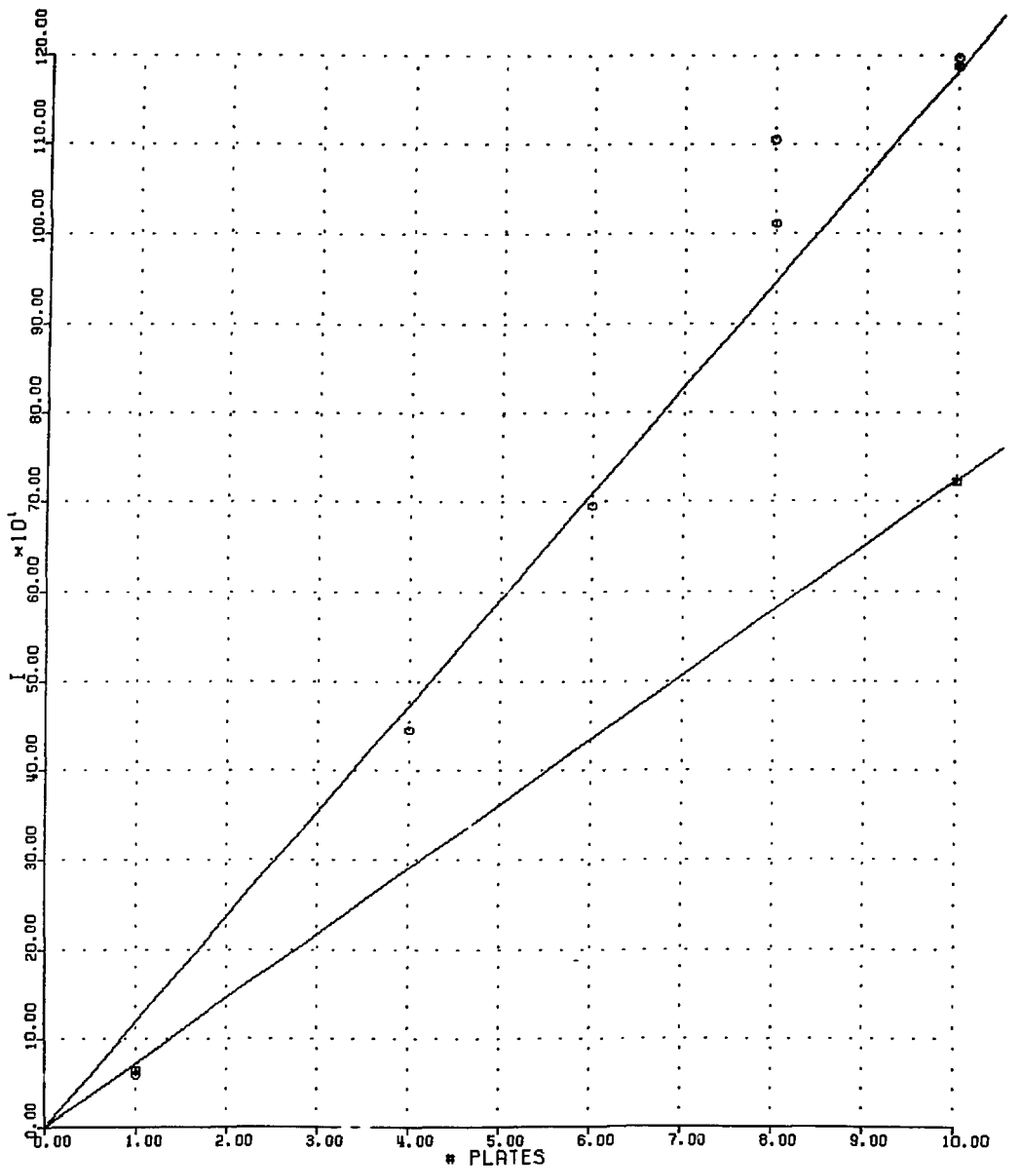

Fig. 5. Count induced by irradiation. The upper curve is the difference between the net active and passive counts for the irradiated plates used in our experiments, while the lower curve is defined by the similar single point for ten unirradiated plates. Extra lead shielding was used in each case.

shielding. Ten unirradiated plates showed a net passive count of 132.7 ± 10.4 with the additional shielding; these uncertainties are one standard deviation. These plates are not virgin HEU, and the gradual buildup of some long-lived fission product has been suggested as the explanation. On the other hand, an earlier investigation of ^{137}Cs, for instance, showed the amounts used to give no detectable passive response in the RD.

A useful safeguards method may not be derived until the measurement values are clearly shown to be independent of fission-product gamma interference. We have concluded that the addition of lead shielding is not such a method.

B. Gamma-Gamma Coincidence Rejection

A Texas Nuclear version of the LASL random driver was used for this work.[3] The instrument electronics was arranged in a coincidence time-overlap spectrometry mode.[4] Here, time-overlap information available at the output of the fast coincidence module is used to separate gamma-gamma coincidence events from n-n coincidence events. Basically, following a fission event, gamma-gamma coincidences occur before n-n coincidences and, therefore, may be electronically rejected from the net coincidence count.

The result of this work paralleled that of the attempt to shield the fission-product radiation with extra lead; that is, the time-overlap method helped, but did not eliminate entirely the adverse effects. Our

conclusion is that a measurement system built around plastic scintillator detectors is far too sensitive to gamma radiation to allow practical measurements on irradiated fuel.

VII. DISCUSSION--THE METHODS IN PERSPECTIVE

The objective of this task was to evaluate NDA techniques for safeguards application to FCA storage facilities. Two straightforward methods have been found useful in this regard--namely, the performance of passive gamma measurements and/or the performance of active coincidence interrogation. Both of these methods may be applied to the verification of FCA fuel while it is in specially designed canisters. Also, both methods may be applied in an inventory situation with minimum facility impact.

It is our intent to apply both NDA methods to an existing FCA facility at Argonne. The objective is to arrive at a point where the HEU plate inventory is secured under a viable safeguards verification plan. To do this, we will perform some or all of the following sequence of operations:

1. The verifying of the enrichment of each plate individually with a rapid gamma measurement.

2. The repackaging of all HEU plates currently in storage into new storage canisters, carefully noting the plate count in each canister.

3. The weighing of the uniquely identified canisters and the obtaining and recording of the weight measurements for each canister.

4. The attaching of TID's on both the inner and outer portions of the storage canister, and the recording of all seal numbers.

5. The performing of the scan.

6. The performing of an active interrogation of each can with the random driver.

7. The return of each canister to an identifiable storage location in the vault.

8. The establishment of a sampling plan.

All data collected is to be stored in a systematic, retrievable manner on a computer dedicated to safeguards purposes. A detailed measurement procedure is to be written for each NDA method and should include a description of the method, of the calibration and application procedures, and of the typical performance of the method. Rules based on some statistical methods will be included for accepting or rejecting canister count data.

On a practical basis, the problem of recently irradiated plates is expected to be of little consequence because records of typical FCA operation show relatively little transfer activity of such plates

between vault storage and reactor over the long term. This means that a small number of instances are expected where the random driver method will not apply. These instances may be readily detected by first performing a passive count of the canister and then comparing this count with that from a known unirradiated-plate canister.

With the inventory "baseline" established as described, a diversion alarm could start the following sequence of verification actions:

1. The weighing of each canister and the checking of the external TID, comparing weight and TID number with computer-stored data.

2. The performance of a passive gamma scan of each canister and the comparing of the integrated 185-keV photopeak peak value with the recorded value for that container.

3. Concurrent with the gamma scan measurement, the performance of an active interrogator measurement of a statistical sampling of the storage canister.

(Specific verification actions taken would, of course, depend on the nature of the alarm.)

The objective in a diversion-alarm situation is to determine as rapidly as possible whether or not a diversion on the order of 25 kg of highly enriched uranium has taken place. Canisters that yield count data outside the acceptance levels would be opened for a more critical examination that included a plate count and individual gamma-ray examination.

REFERENCES

1. J. Blachot and R. de Tourreil, "Table of Gamma Rays from Fission Products," J. Radioanal. Chem. II (1972).

2. S. B. Brumbach, et al, "Fast Critical Safeguards, Summary Report," Argonne National Laboratory Report ANL-80-13, Vol. II, (1980).

3. J. E. Foley, Los Alamos Scientific Laboratory Report LA-4883-PR (1972), pp 9-12.

4. Texas Nuclear System Manual.